Automated Enclosure and Protection System for Compact Solar-Tracking Spectrometers

Ludwig Heinle[1] and Jia Chen[1]

[1]Environmental Sensing and Modeling, Department of Electrical and Computer Engineering, Technische Universität München, Munich, 80333, Germany

Correspondence to: Jia Chen (jia.chen@tum.de)

Abstract. A novel automated enclosure for protecting solar-tracking atmospheric instruments was designed, constructed, and successfully tested under various weather conditions. A complete automated measurement system, consisting of a compact solar-tracking Fourier Transform spectrometer (*EM27/SUN*) and the enclosure, has been deployed in central Munich to monitor greenhouse gases for one and half years and has withstood all critical weather conditions, including rain, storms, and snow. It has provided ground-based measurements of column-averaged concentrations of CO_2, CH_4, O_2, and H_2O throughout this time.

The enclosure protects the instrument from harmful environmental influences while allowing open path measurements in sunny weather. The newly-developed and patented cover, a key component of the enclosure, permits unblocked solar measurements, while reliably protecting the instrument. This enables dynamic decisions about taking measurements, and thus increases the number of data samples. This enclosure leads to a fully automated measurement system, which collects data whenever possible without any human interaction. In the long term, the enclosure will provide the foundation for a permanent greenhouse gas monitoring sensor network.

1 Introduction

Anthropogenic greenhouse gas (GHG) emissions into the atmosphere have risen to a worrying level over the last few decades. There is little doubt that this impacts the climate on earth and eventually the well-being of humanity. To understand greenhouse gas sources, sinks and transportation, reliable and precise atmospheric concentration measurements are required. State of the art ground-based and space-borne spectrometers are used to measure column-averaged gas concentrations by analyzing the gas absorptions for specific frequencies of sunlight. Ground-based solar-viewing spectrometers use the sun as a light source. Gas molecules, such as O_2, CO_2, and CH_4, interact with the sunlight on its path through the atmosphere, resulting in absorption lines in the recorded sun spectrum. By observing the intensity attenuation of light at specific frequencies, the concentration of gas molecules within the air column can be determined.

The Total carbon column observing network (TCCON) (Wunch et al. (2011); Toon et al. (2009)) is a global network that measures total column concentrations. The instruments deployed in the network are *Bruker IFS 125HR* spectrometers, which provide accurate data to validate satellite observations. However, these instruments are large (close to 2x3m footprint), weigh

more than half a ton and are expensive (Bruker Optic GmbH (2006)). Further, their operation is costly in terms of staffing. Therefore, many working groups operating *125HR* spectrometers use remote control or automated systems for operation. A team at the *Belgian Institute for Space Aeronomy* developed *BARCOS* (Neefs et al. (2007)), which stands for "Bruker automation and remote control system". Later, Geibel et al. (2010) developed an automated system to deploy the *125HR* on Ascension Island. The main goal of these systems is to lower the operational costs by reducing the need for local human interaction for operation. However, operation of a *125HR* still requires regular skilled on-site maintenance, due to the degradation of interferometric alignment over a time scale of months (Hase (2012)).

A portable solar-tracking FTIR spectrometer, the *EM27/SUN* (Gisi et al. (2011, 2012); Hase et al. (2016)) has been employed for many applications in urban greenhouse gas emissions studies in recent years. It is lightweight, compact, and very robust and has attained a comparable precision to TCCON instruments (Frey et al. (2015); Hedelius et al. (2016); Chen et al. (2016)). It is easy to transport and operate, and therefore permits a more flexible site selection. While the large *125HRs* are deployed for global observation, the small *EM27/SUN*s are more often utilized for local and city source investigations (Hase et al. (2015); Chen et al. (2016); Franklin et al. (2016); Viatte et al. (2017); Chen et al. (2017); Toja-Silva et al. (2017)). Further, it has been deployed on a ship (Klappenbach et al. (2015)) and in a mobile observatory to assess volcanic emissions (Butz et al. (2017)). The *EM27/SUN* is equipped with a solar-tracker unit, consists of motorized rotating mirrors to direct the light into the spectrometer. An external laptop is connected to the spectrometer via multiple connectors. Even though the *EM27* body itself is weather resistant, the other components, e.g., the laptop, the control electronics, the solar tracker, and especially the tracker mirrors need to be protected. Hedelius et al. (2016) found degradation of the solar tracker mirrors in their spectrometer, which could have been caused by a combined action of reactive substances, sea-salt aerosols, and humidity above saturation, in which case the contaminated water droplets might be deposited on the mirrors.

Much human effort is necessary to operate the instrument at a measurement site. A person needs to set up the system every time before measuring. This setup needs to be manually dismantled and stored safely, whenever the weather changes to rainy or stormy conditions. Besides wear and tear of the connectors, much costly labour is necessary. Even though the operators do not need to be highly trained, their permanent attention is required. Consequently, a very limited availability to measure during short periods of good conditions reduces the amount of data collected.

We have developed an automated enclosure (Figure 1) that houses and protects the measurement system, while allowing measurements during good weather conditions. It eliminates the need to dismantle the system after each measurement period, and protects against harmful weather conditions. A remote operator can monitor multiple stations simultaneously, while the setup and dismantling times can be reduced to a minimum. The easy handling combined with the small size and low power consumption reduce operational costs of such a measurement system to nearly zero.

To construct such an enclosure, several challenges must be faced. A safe and reliable protection against environmental influences, like dirt, thunderstorms and even hail, is needed for the measurement system, though it is necessary for the sun tracking mirrors of the instruments can be directly exposed to the sunlight during sunny weather conditions. Therefore, the prime directive for the enclosure design is reliable protection and maximized amount of measurement data. Other criteria include the best possible remote controllability via the internet, the thermal stability of the system, as well as a stable and

uninterrupted power supply. The latter ensures error free collection of the data and prevents the system from unpredictable situations. To conclude, the enclosure is designed for automatic operation without the need for human interaction.
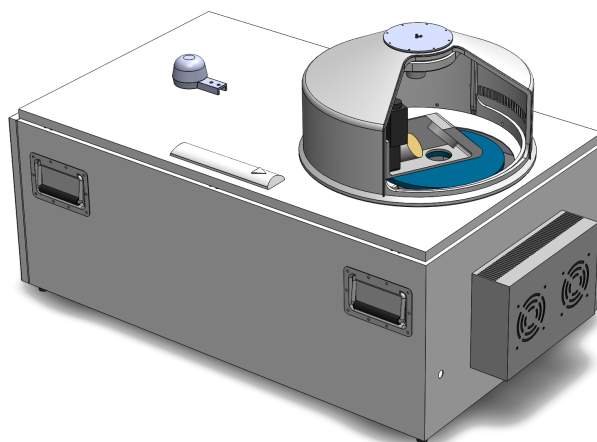
Figure 1. 3D Computer-Aided Design (CAD) model of the enclosure including the base cabinet, the cover, the thermal electrical cooler, and the rain sensor. These hardware components are explained in Section 2.

2 Hardware and Setup

An overview of the components of the automated enclosure is provided in Figure 2 and its dimension and weight are given in Table 1. These components are explained in the following subsections.

Overall Dimension	112 x 62 x 66 cm	(length $\times$ width $\times$ height)
Base Enclosure Dimension	112 x 62 x 41 cm	(length $\times$ width $\times$ height)
Cover Dimensions	45.5 x 25 cm	(diameter $\times$ height)
Total weight (spectrometer included)	$\approx$ 100 kg	

Table 1. Dimensions and weight of the enclosure.

2.1 Base Cabinet

As previously mentioned, the *EM27/SUN* spectrometer requires physical protections. Therefore, a stable and waterproof control cabinet is placed with its opening facing up and serves as the base cabinet for the enclosure. In this orientation, the door is located on top and allows easy access to all equipment inside. Rubber feet on the bottom ensure a slightly elevated stable position. The electrical components of the enclosure, such as power distribution and power supplies, are attached to a DIN-rail. All wiring is stowed in cable ducts to keep the inside neatly organized, easy to access and reliably operating.
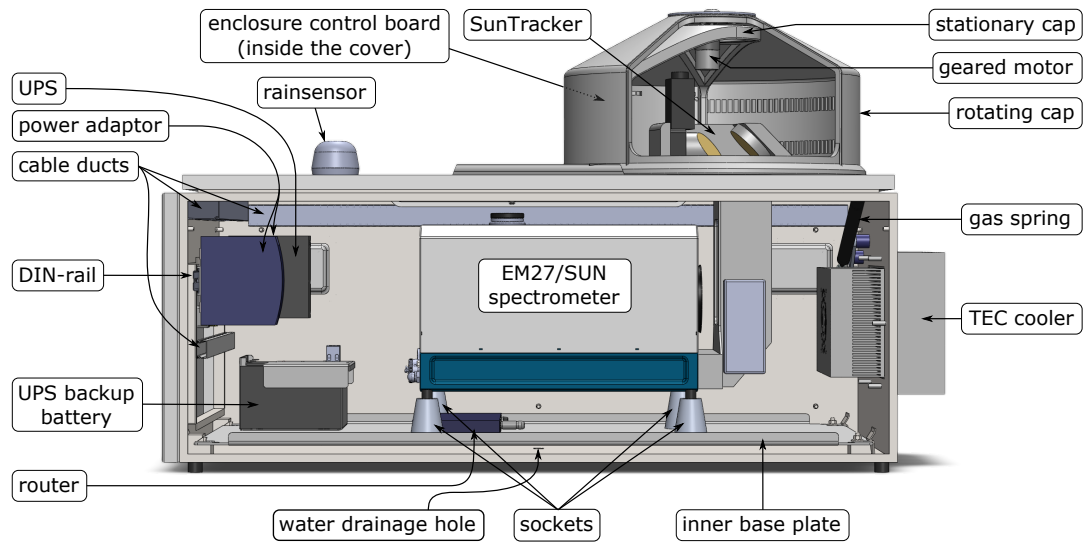
Figure 2. Enclosure overview: components and their arrangements. The Laptop is placed on top of the EM27/SUN spectrometer to ensure a good accessibility.
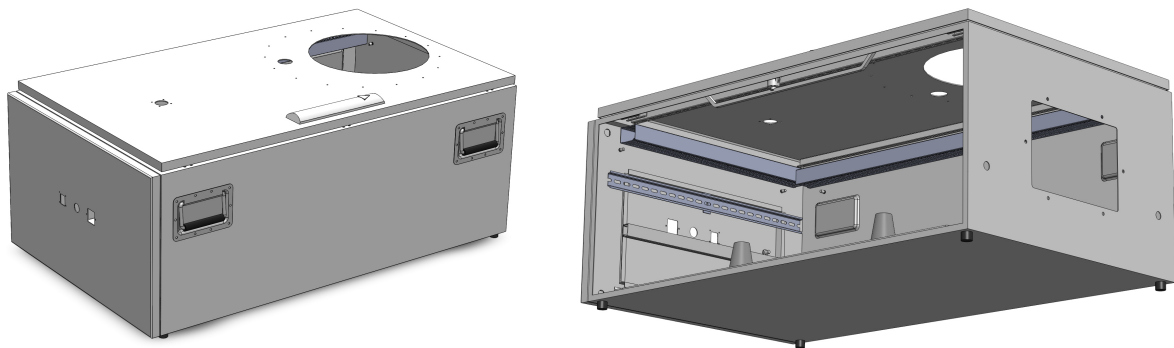
Figure 3. 3D-Model of the base cabinet. In the left figure the original function as a control cabinet is clearly identifiable. The handles on the side wall are mounted for easy transportation. The right image shows another perspective, with one of the side walls removed to allow a view inside the empty base cabinet.

The base cabinet depicted in Figure 3, is manufactured of steel. Thus, it is very strong and durable. Four handles, one on each corner, allow easy transportation. The measurement system comfortably fits inside and is well protected by the base cabinet. The upper end of the solar-tracker, which rises through an opening in the base cabinet, is the only part of the measurement system located outside. A cover, as described in Section 2.2, is mounted over the opening, to close the enclosure and protect
5 the instrument.

2.2 Cover

Because the solar-tracker extends through the top of the base cabinet, it must be protected separately against harmful environmental influences. Tests with a glass dome were performed at the Karlsruhe Institute of Technology (KIT) (cf. Sha (2015)). Unfortunately, the results were not as good as expected, since it was not possible to manufacture a dome with a sufficient homogeneously surface. The sunlight was variously distorted depending on the solar incident angle, which affected the measurements. Moreover, dirt and dust on the glass surface as well as trapped humidity inside the dome could further disturb the measurements.
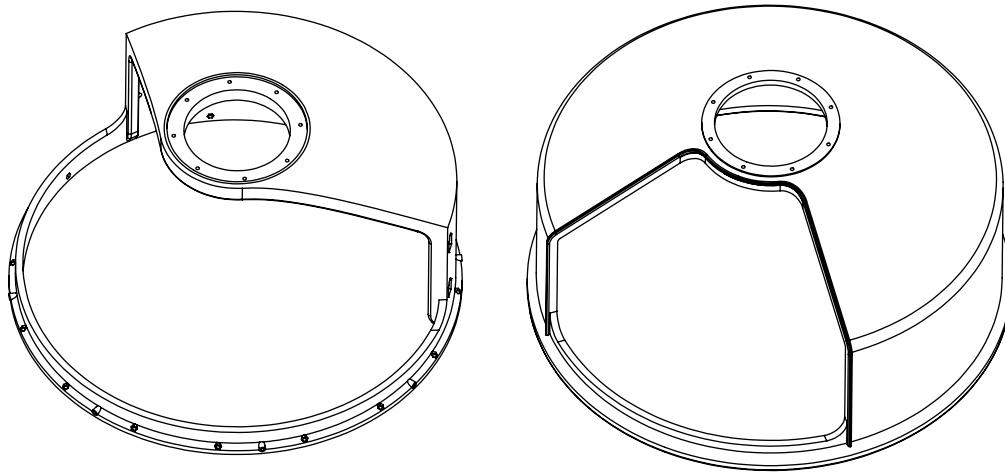
Figure 4. Drawings of the two parts of the cover. The inner cover with its large opening is depicted on the left. The cover on the right is the outer one with a relatively small cutout.

2.2.1 Cover Design

A completely different concept is presented here. A newly developed and patented cover is mounted on top of the opening, covering the solar-tracker. The cover is made of two rotationally symmetric parts with cutouts, where one fits inside the other (c.f. Figure 4 and Figure 5). It protects the solar-tracker from bad weather while enabling open path measurements in dry and good weather conditions.

The outer cover rotates about the vertical symmetry axis on top of the inner cover. Its weight is carried by eight ball bearings equally distributed around the lower end of the inner cover. While the inner cover is mounted in a stationary position on top of the base cabinet, the outer one rotates. The rotation is driven by a simple geared electric motor, which is mounted inside in the common axis of the two covers.

2.2.2 Cover's size

The dimensions of the cover is given in Table 1. The lower size limit of the outer cover's opening is determined by the width of the mirrors. Since sunlight must not be blocked during sunny conditions, and the sun rays can be assumed to be parallel, the opening must be at least the width of the mirrors. However, in this case the cover needs to track the solar azimuth angle very precisely during the course of the day, so that it does not block the sunlight from the mirrors. Furthermore, the smaller the opening is, the more difficult the accessibility inside the cover is for any maintenance.

The upper size limit for the opening is determined by the size of the inner cover's remaining wall. During bad weather conditions or darkness, the outer cover will rotate to a closed position where the inner cover wall needs to be fully covered by the opening of the outer one. Sealing concerns and a lower demand for positioning precision led the design towards greater overlap. Finally, an opening of 90° was considered to be a good trade off between overlapping and necessary tracking accuracy for the first prototype.

A rough estimation based on the 3D CAD model shows that the permissible solar zenith angle range is $23(\pm1)°$ to $88(\pm1)°$. From test results (c.f. Section 4.2) and the model, we determined the azimuthal range is from 71° to 300°. The cover was designed to be deployed in Munich, so for other places on earth, a redesign of the cutouts might be necessary. This redesign can be carried out with a simple modification of some parameters in the 3D-Model, which was made to design the enclosure.

2.2.3 Weather Proof Concept

Figure 5. The image shows the gaskets that were installed to seal the gap between the two covers, preventing water from being blown into the cover by strong winds.

A gap between the two covers ensures a friction-free smooth rotation of the outer cover. However, rain combined with strong winds could blow water into the cover despite the overlap between the inner and outer covers. Thus, a gasket as depicted in Figure 5 has been added to the cover. It is a window sealing strip that has been cut to the right thickness. When the cover is

closed, the gasket blocks the wind and thus prevents water from entering. In addition, it fills the gap between the two covers and thus keeps insects from getting inside. Nevertheless, the rubber sealing does not obstruct the smooth rotation of the outer cover.

2.2.4 Position Determination

5 The outer cover needs to track the sun for undisturbed measurements. Therefore, the actual position of the outer cover needs to be determined. To this end, we have developed an encoder using magnets and reed sensors that are placed inside of the notches on the covers (Figure 6). With this concept, the absolute cover position can be determined and the spectrometer is reliably protected.
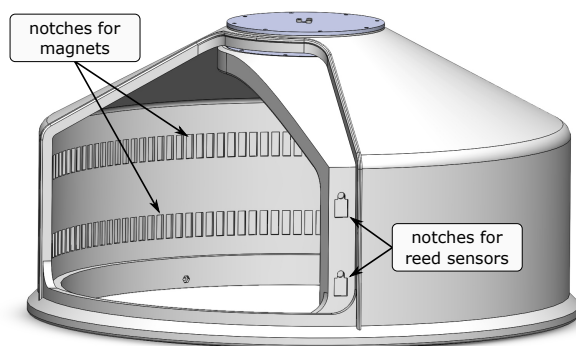
Figure 6. The image shows the cover with notches for magnets and reed sensors to track the outer cover's orientation.

Three reed sensors are glued in the notches of the inner cover, and each of the sensors has an electrical contact that closes
10 if the sensor is exposed to a magnetic field. Nineteen neodymium magnets with a magnetic flux of 1.17 Tesla each were distributed in the notches of the outer cover. One reed sensor and a single magnet positioned in the upper notches are used to detect the closed position (absolute zero position). From then on, the motion direction is determined and the number of magnets are counted. The position can be determined with a precision of about $10°$.

To assess the distance and direction of any movement, two more reed sensors are installed next to each other in the lower
15 notch of the inner cover. Whenever a magnet passes by the sensors, one sensor will act a little earlier than the other. This delayed operation can be used to determine the direction of movement. Multiple magnets are distributed with alternating polarity around the outer cover opposite to the two sensors. Alternating the magnetic polarity creates a very weak field between two magnets as shown in Figure 7b. Compared to this, if the magnets were placed with the same polarity, the magnetic field strength would not vary significantly among the magnets as depicted in Figure 7a. Since the reed switches are sensitive to the magnetic field
20 strength and not the polarity, this alternating arrangement ensures the sensors operate reliably.

To make sure that the sun path to the tracking mirrors is never blocked, the mirrors' azimuthal orientation is read directly from the mirror control. The corresponding position for the outer cover is determined and set as the target position for the cover's control unit.

(a)   (b)
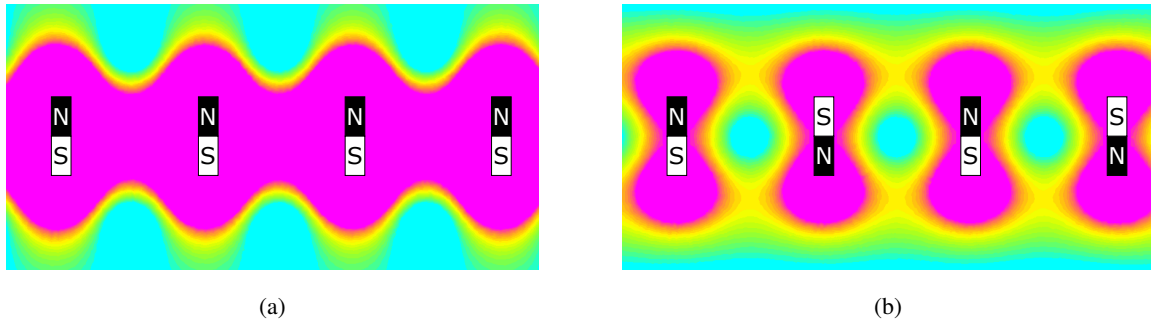
Figure 7. Comparison of the magnetic field strength when placing the magnets in the same polarity (a) and alternating polarity (b). Cyan represents a weaker magnetic field, whereas pink represent a stronger field.

2.3 Thermal Regulation

There are several thermal concerns regarding the *EM27/SUN*. For instance, the sun tracker's stepping motors may stall in freezing temperatures, possibly due to greasing. Another point is the unknown impact of heat on the system. Inside the *EM27/SUN*, an InGaAs-detector senses the intensity of the NIR-light coming out of the interferometer. Typical InGaAs-detectors have a temperature-dependent transfer function (K.K. (2015); LLC (2004)), which means they function best with a constant operating temperature. Further, condensation needs to be prevented. When warm air hits cold equipment, water vapor in the air will condensate on the cold surfaces of the equipment and tracking mirrors, which can distort the data, damage the electronics, or even potentially cause mirror degradations. A ventilation system combined with an electric heater was considered as a solution, but this has several downsides. First of all, high humidity may be vented into the enclosure, necessitating an air dehumidification system. Furthermore, a number of openings would be necessary for the ventilation, increasing the risk of leaks for rainwater and small animals to enter the enclosure. Finally, much heat may escape driven by wind blowing through ventilation openings when heating is needed.

Thus, another much easier approach that even offers cooling below the outside temperature was chosen. A thermoelectric cooler (TEC), using a solid-state Peltier device, has been installed at one of the walls of the base cabinet. The TEC-element is controlled by electrical current and transfers heat energy into or out of the enclosure. It does not require holes for ventilation and therefore keeps the enclosure waterproof as well as closed to animals. Further, by maintaining the temperature inside the enclosure between 24°C and 25°C, condensation can be avoided.

To prevent an unintended heat exchange between the inside and outside of the enclosure, thermal insulation is installed. A 13 mm layer of special foam with a very low thermal conductivity, less than $0.040\,\mathrm{Wm^{-1}K^{-1}}$, covers the inside of the base cabinet, allowing a low heat transport even on high thermal gradients between the inside and the outside.

Because the enclosure houses many heat sources, cooling represents a greater challenge than heating. The power necessary for cooling is calculated by the given values of the components' specifications in their data sheets. A maximum average power of about 120 W (see Table 2) must be transferred out of the enclosure. The specification of the selected TEC lists a cooling

Component	max. Power
Spectrometer with solar-tracker	45 W
Laptop	30 W
Power supply and UPS	35 W
Router, Voltage converters, etc.	~ 10 W
Total	~ 120 W

Table 2. The table shows the expected maximum average power dissipation of all components inside the enclosure.

capacity of 135 W. Thus, about 15 W of extra cooling power will be available. Equation 1 is a rough estimate of the thermal diffusion. It shows that the cooling system can sufficiently cool the inside to about 2 K below the outside temperature.

$$\Delta T = \frac{\dot{Q}l}{\lambda A} = \frac{15\text{W} \cdot 13\text{mm}}{0.040\text{Wm}^{-1}\text{K}^{-1} \cdot 2.48\text{m}^2} \approx 1.97 \text{ K}, \tag{1}$$

where $\dot{Q}$ stands for the thermal power to be transported along the distance l. A is the area of the thermal conduction and λ is
5   the thermal conductivity of the material within the volume $A \cdot l$.

2.4 Rain Sensor

A *Hydreon RG-11* optical rain sensor is installed on top of the enclosure next to the cover. When rain is detected, the integrated logic of the enclosure will automatically close the cover and send a message to the measurement system. This message may stop ongoing measurements or inform an administrator.

10   The sensor works as follows: an infrared LED emits light into a dome-shaped lens. The light is reflected by the lens surface and travels along its shape to the other side where it strikes a photodiode, which monitors the light intensity. When a water drop lands on the surface of the lens, less light will be detected by the photodiode because the drop allows the light to escape by refraction. RG-11 was chosen due to its dome-shaped surface. It is an improvement over a flat surface as the drops do not accumulate on the surface, which could produce a false signal after the rain stops.

15 ## 2.5 Gas Spring

As described in Section 2.1, the enclosure's design is based on a control cabinet. In an upright position, the cabinet's door can easily be accessed and will stay in any position the user leaves it. Hence, it is not equipped with any door openers or springs. In this application, the cabinet's orientation is changed, so the door is now located on top. Therefore, the door's open positions are no longer stable and gravity will always push the door down. Hence, a gas spring has been added to the door.

20   A very simplified model, shown in Figure 8, is used to properly position and dimension the gas spring. The gas spring is designed such that it does not close on its own at any position. Thus, an operator can never be injured by the door dropping. The damping of the gas spring is very strong, so that any movement is curbed to very slow speed. Additional damping at the
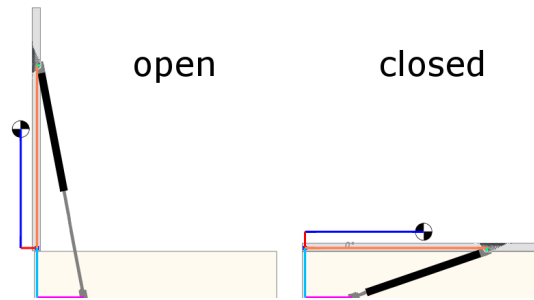
Figure 8. Simplified model of the base cabinet and its door to calculate the joint positions and the strength of the gas spring.

end positions ensures extra low acceleration, so that the cover will not be subject to strong impacts at those positions. The gas spring has a length of 582 mm and a maximum travel of 250 mm. Its pushing force is about 180 N, which is sufficient to lift the 15 kg door. The maximum force at the joints is calculated as 270 N.

2.6 Uninterruptible power supply

As previously mentioned, an electric motor rotates the outer cover. There is no mechanical fallback that can close the cover in case of a power outage. Hence, an uninterruptible power supply (UPS) is mandatory. Additionally, temporary power outages will destroy measurements and may place the system in an undefined state; therefore, the UPS is designed to supply sufficient energy to the measurement system for several minutes.

2.7 Relays

While operating the *EM27/SUN* in the past, occasionally unexpected errors occurred, some of which could only be resolved by restarting the spectrometer or its camera. Thus, two relays are included so that a remote operator, or a controlling software, can switch off the power to the spectrometer as well as disconnect its USB-Camera from the laptop.

The first relay is mounted on the DIN-rail and connects the power to the *EM27/SUN*. Besides resolving errors, this switch allows powering the instrument off at night and thus helps to save energy. The second relay is located on a USB-intermediate-plug. It was developed to enable the solar-tracker USB-camera to be disconnected. In the past, the only effective solution to recover from camera errors is to physically reconnect the camera. Therefore, the relay on the intermediate-plug simply disconnects the 5V wire of the USB-connection, which simulates the physical unplugging of the USB-connector. As long as the relay is closed, the USB-data-communication will not be affected, since the data lines of the USB-connection remain untouched. With the help of this circuitry, the USB-camera can be reset by a remote operator or automatically by a software.

2.8 Enclosure Control Board

The control board of the enclosure handles low level access to the enclosure's hardware. It provides protective safety features, like closing the cover whenever an error occurs. Furthermore, it receives commands from the laptop and operates the enclosure

hardware accordingly. The control board works independently to guarantee a very high level of fail safety. Almost every signal on and off the board is designed for the highest possible fault tolerance to ensure reliable operation in every situation.

The control board implements the most critical safety features and serves as a tool for the laptop to operate the enclosure. The central brain of the board is an *Atmel ATmega168* microcontroller. The system on chip (SOC), which includes a small,

5   20MHz RISC[1] processor with integrated memory, is very robust. Besides a crystal and some capacitors, no external hardware is required, which makes the control board very reliable. For the communication with the laptop, an *FTDI FT232RL* USB to RS232 converter is placed on the board. More details on the operation of the Enclosure Control Board and the communication interface are given in Section 3.1.

3   Software

10   ### 3.1   Enclosure Control Board Software

The enclosure control board is a central component of the enclosure. The software for the microcontroller on that board implements the enclosure's basic logic, driving and controlling the electric motor of the cover and reading its position by evaluating the signals of the sensors in the cover. Moreover, it receives the signals of the rain sensor and UPS and communicates with the measurement system via USB. Controlling some relays, the enclosure control board can even power up or power down

15   the spectrometer inside the enclosure. Self-monitoring and a fail-safe circuit design guarantee high reliability and security, ensuring full control and best protection of the instrument inside.

3.1.1   Structure of the Software

To exploit the limited hardware resources as much as possible, the software is split into a set of high and low priority tasks. The most important high priority task is the control of the cover as explained in Section 3.1.2. The low priority tasks are the

20   less time-critical, communication processes. Resetting the hardware watchdog is also classified as low priority.

Figure 9 shows a full overview of the program flow. The reset node is the starting point of the program after every reset. After that, the processor initializes and enters its main loop, where it executes all the low priority tasks. An interrupt will be executed every 10 minutes, processing the high priority tasks.

3.1.2   Cover Control Scheme

25   Figure 10 depicts the cover control flow. While operating in normal mode, the drive controller compares the current position to a target value, which can be derived from the azimuthal orientation of the tracking mirrors or the closed position. Depending on the distance between the two orientations, a target speed is calculated and fed into a ramp generator that slowly accelerates or decelerates the rotation of the cover to reduce mechanical stress. Its output signal controls the motor driver. The current

---

[1]Reduced Instruction Set Computer
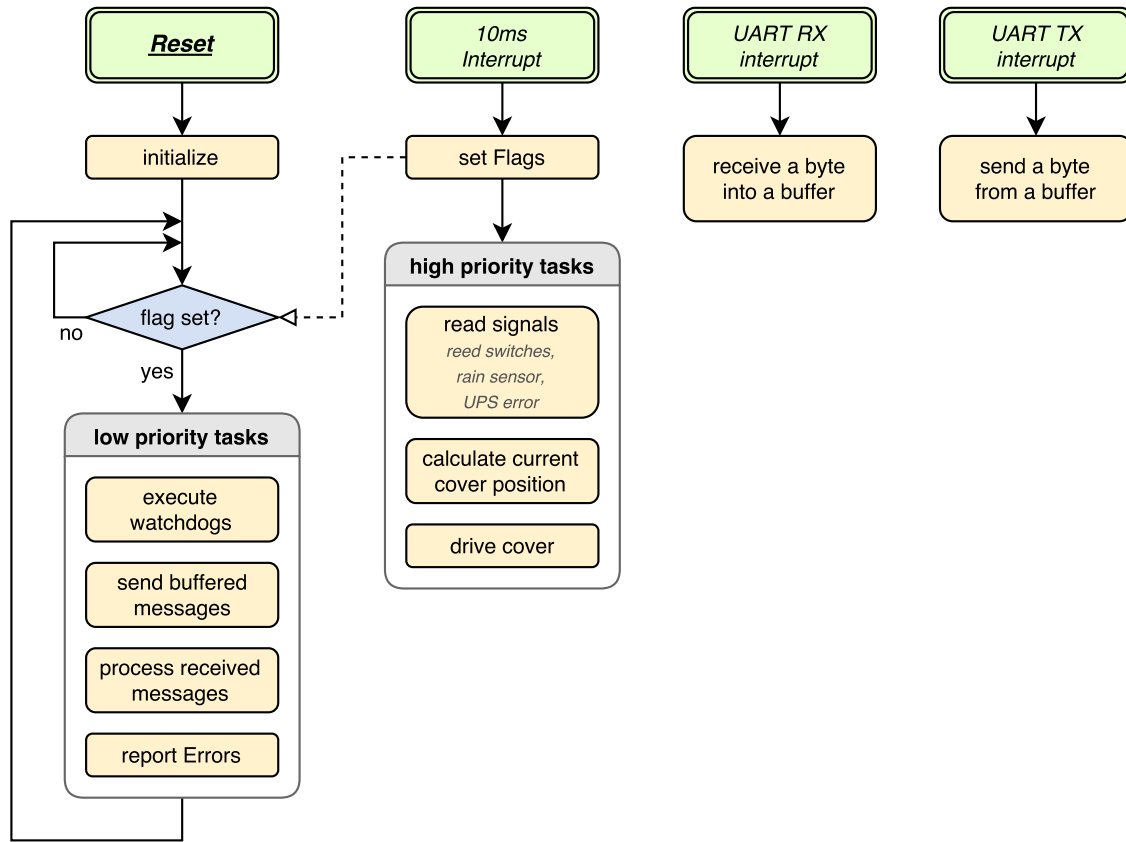
Figure 9. The flow chart visualizes the structure of the microcontroller's software.

position of the cover is calculated from the sensor readings and fed back to the drive controller. In case of any error, the target position will be set to the closed position, as explained above.

An additional forced mode is included to allow full control in case of emergency. If an error occurs, the loop can be cut open via the interface, and a fixed value can be fed into the ramp generator. Hence, a remote operator can take full control of the cover and navigate it into a secure position if needed.

3.1.3 Safety Features

The microcontroller's hardware includes a watchdog feature that monitors the processor's operation. A watchdog is basically a timer that expects a reset signal in its configurable period. In normal operation the watchdog timer will be reset before a timeout occurs. However, if the processor gets hung at any position in the program, the watchdog timer will time out and consequently trigger a full reset, guaranteeing a very high reliability of the operation.
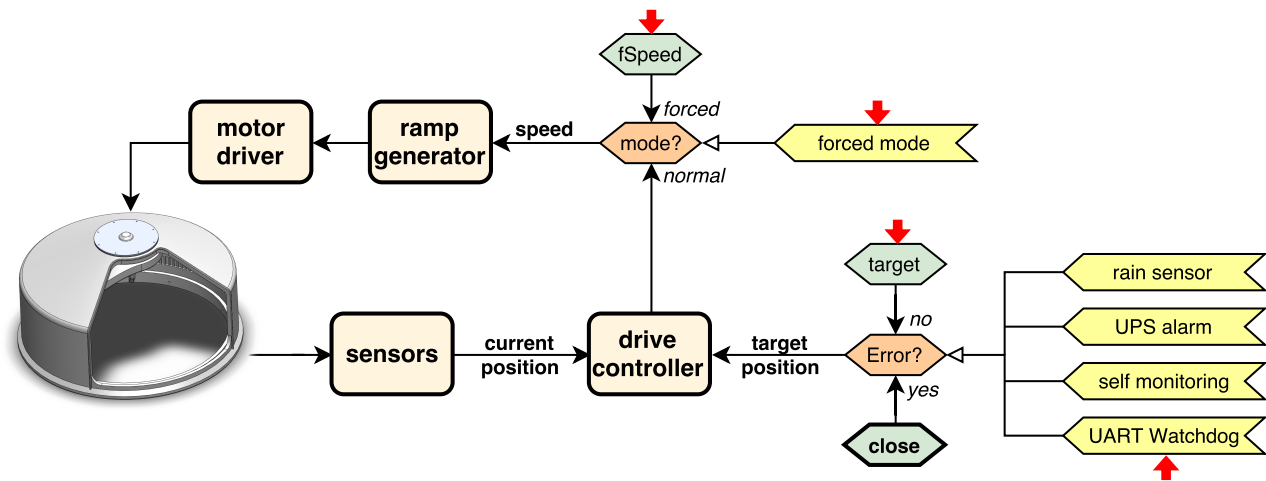
Figure 10. The flow chart shows the design of the cover control flow. The red arrows indicate values that can be changed or influenced by the user via the USB-interface.

Additionally, the software provides an optional UART watchdog. When enabled, it will expect an alive message every 5 seconds. In contrast to the hardware watchdog, which is not optional, a timeout of the UART watchdog will not trigger a system reset. Instead, an error-flag will be set and the program will close the cover (see Figure 10).

3.2 Computer Software

We also developed a computer software, programmed in python, to offer a set of methods to control the enclosures functionalities with a graphical user interface (GUI). The GUI is called *ECon*, which is short for "Enclosure Control" and appears as a window on the desktop (Figure 11).

4 Results

After constructing the enclosure, its functions were tested. First of all, the dryness inside the enclosure after extreme stormy and snowy condition is confirmed. Secondly, the ability to regulate the temperature inside the enclosure is examined. Next, we investigate whether it blocks the sun during the course of the day. Finally, the remote controllability and operability are shown.

4.1 Rain and Snow Test

Several extreme weather conditions acted on the enclosure. The surveillance camera, which has been installed to allow a remote live view of the enclosure, captured the stormy condition in Figure 12. Even after these extreme rainy and windy conditions, the enclosure remained completely dry inside and not a single drop of water penetrated it. Figure 13 shows that no water was
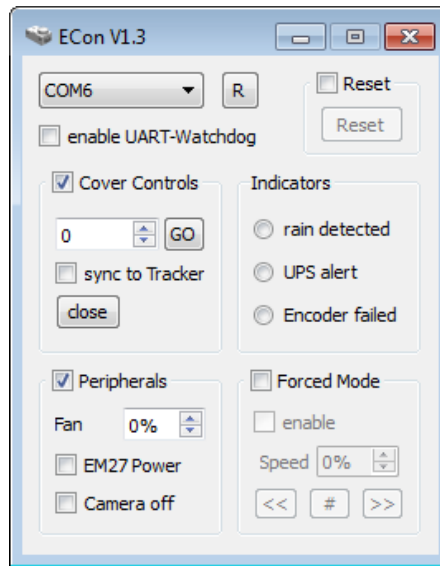
Figure 11. The image shows the graphical user interface called ECon. With the given controls and indicators, nearly every enclosure function can be controlled and observed.

blown into the cover. The rain sensor also reliably detected the first drop of water on its sensitive area and the cover was closed in less than 6 seconds.
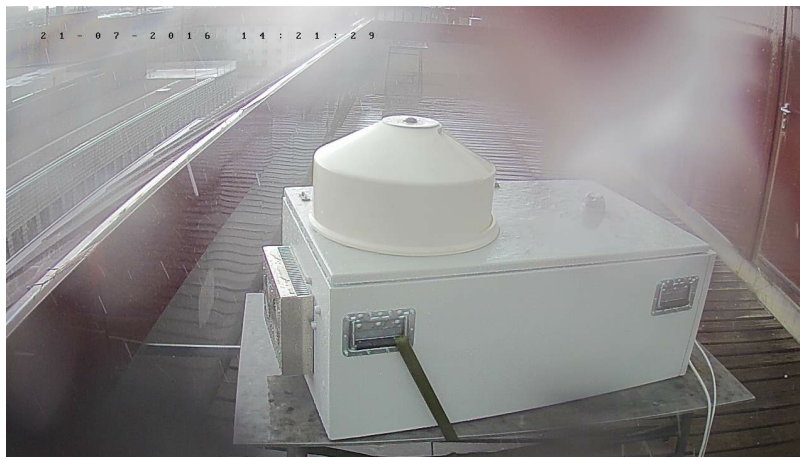
Figure 12. Impression of the bad weather the fully equipped enclosure was exposed to.

In winter 2016, Munich experienced a lot of snow, and the enclosure proved to be robust against snowfall on the cover (Figure 14). The enclosure is constantly heated and the spectrometer is able to carry out measurements whenever it is sunny,

Figure 13. (a) Image of flooded stair house. The water was blown into the tilted window. (b) Image of the open enclosure after the storm. As can be seen, no water was able to penetrate the cover.

even if the ambient temperature falls below 0°C. In addition, no freezing occurred. The enclosure is heated to 25°C. The warm air rises up and prevents freezing of trapped water.

4.2 Unblocked Sunlight

During the one year test period, the enclosure showed no single case of blocking the sun during measurements. The test azimuthal angle ranges from 71° to about 296° (see Figure 15). On 29 July, the latter angle was checked in the evening. As shown in Figure 15(a), the sun was not blocked at the 296° azimuthal angle (88° zenith). Afterwards, the sun disappeared behind clouds and buildings. Optical investigations revealed that the sun could remain unblocked until close to 300°. On the next day, the sun was unblocked at an azimuthal angle of about 71° in the morning (82° zenith), as shown in Figure 15(b).

4.3 Thermal Regulation

The enclosure's thermal regulation was tested by logging thermal readings of the outside and inside temperatures during normal operation (see Figure 16). As can be seen, the internal temperature of the enclosure does not exhibit a very smooth temperature curve, mainly because of the regulator, which follows a very simple three-point control scheme. If the temperature falls below the configured threshold of 24°C, the TEC is turned on for heating until the temperature rises above 24.1°C. The same is valid for cooling, whereby the TEC is powered for cooling at above 25°C and disabled at 24.9°C. The regulator has only three states: heating, cooling and off. There is no intermediate state, which would allow for a smoother regulation. Thanks to the temperature control, no condensation was observed on the mirrors or other components inside the base cabinet.
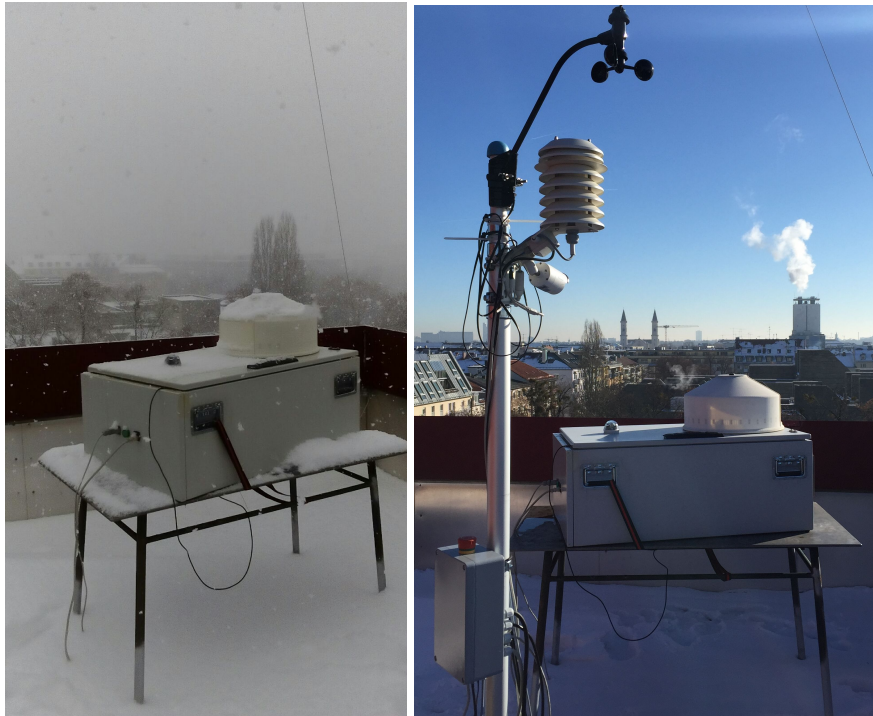
Figure 14. (a) During winter 2016, inches of snowfall on the enclosure with the spectrometer located inside. (b) The system is taking measurements in cold winter below 0°C.

During construction, the TEC was designed to pump out the heat of the measurement system. Cooling below the outside temperature were considered a useful feature after the enclosure was assembled. The built-in reserves of the TEC are not large enough to cool the system more than just a few degrees below the outside temperature (see Figure 16). On 23 July the temperature was controlled within the desired range as long as the outside temperature was lower than 27°C or the measurement system was turned off, such that less heat is generated.

4.4 Remote Operability

The measurement system can be fully operated remotely. Using a remote desktop software, any operator can log in from any computer and take control of the system. Because of the enclosure no physical attendance is required to start, stop or monitor measurements. Figure 17 shows the amount of data collected daily. As can be seen, the density increased clearly when the enclosure was set up for operation. Measurements were taken nearly every day; even small windows in the clouds were used to sample the data.
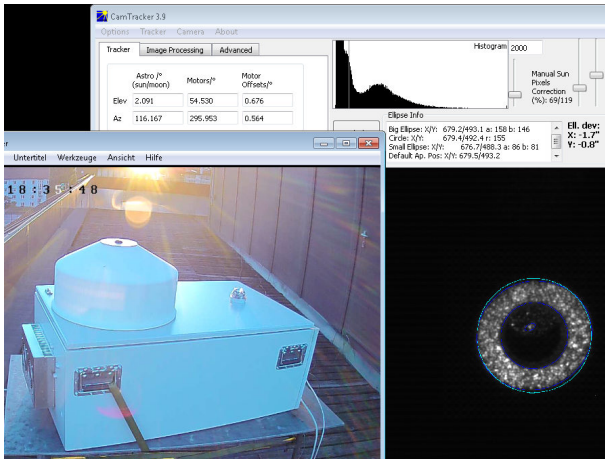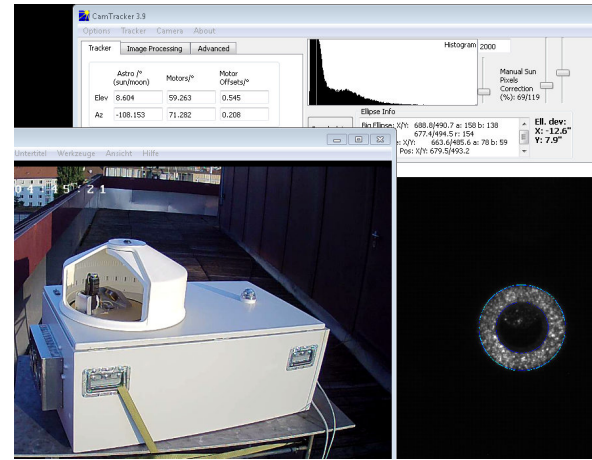
(a)   (b)

Figure 15. The images show screen shots of the laptop in the late evening (left) and early morning (right). The image on the left shows the instrument tracking the sun at an azimuthal angle of 296° on 29 July at 8:35 p.m. local time. The right image shows the tracker following the sun at about 71° azimuthal angle on 30 July at 6:45 a.m. local time. As expected, in both cases the cover did not block the sunlight.
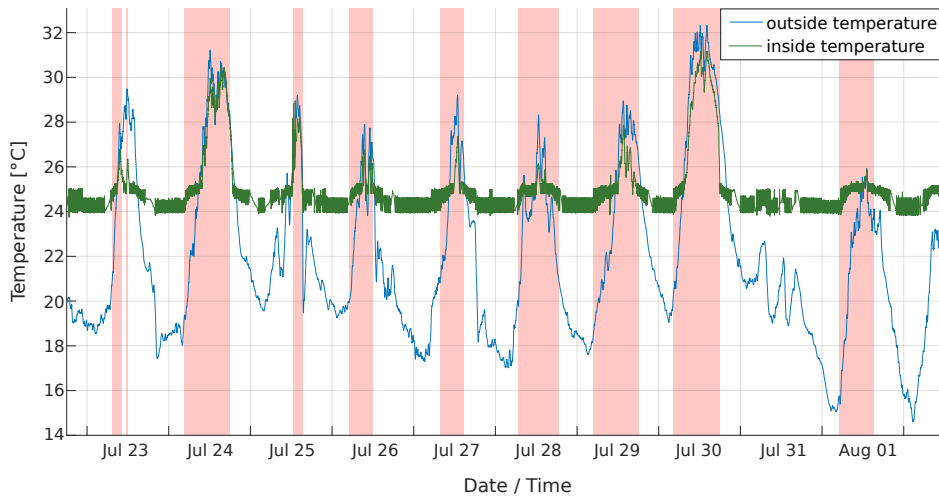
Figure 16. The diagram shows the internal and external temperature of the enclosure. The red bars illustrate time periods during which the measurement system was active and therefore produced heat that had to be pumped out of the enclosure by the TEC.

5 Future Work

In future, rain prediction information can be integrated to assist in the decision making regarding cover control. One potential approach could be to assess real time online rain radar data and meteorological forecasts to predict the upcoming weather situations.
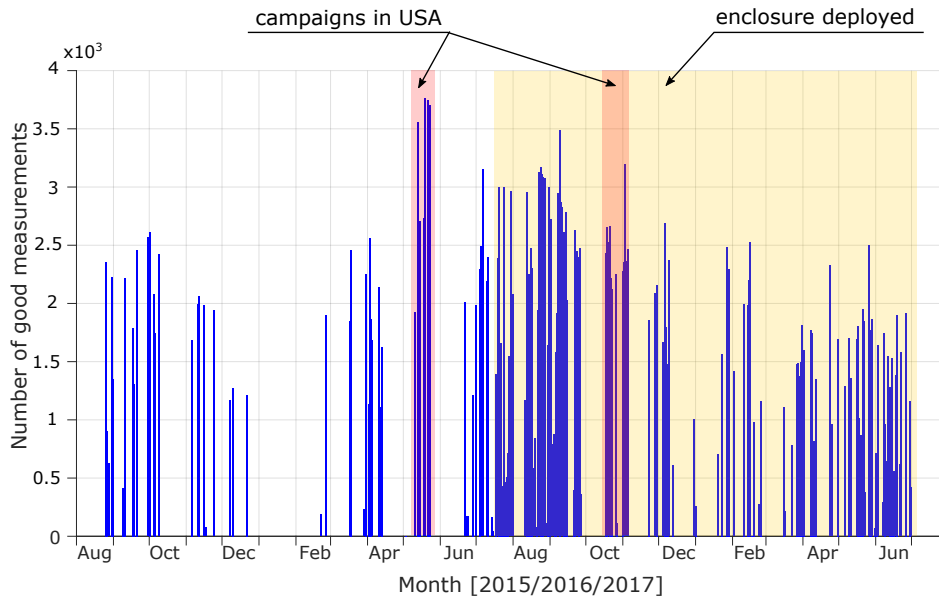
Figure 17. Visualization of the amount of daily sampled data with the *EM27/SUN*. The yellow region marks the time when the *EM27/SUN* was deployed inside of the enclosure. During the time periods indicated by the red regions, the *EM27/SUN* was participating in the measurement campaigns in USA, Indianapolis and San Francisco Bay Area, respectively. Due to the shipping time to and back from the USA, the measurements were not taken a month before and after the campaigns.

Further improvements of the enclosure could focus on a localized thermal regulation. One could specify the most sensitive components of the measurement system and pay particular attention to their thermal regulation, which could also meet the thermal demands while reducing the total energy consumption.

Another enclosure improvement could target a lightweight and portable version, which would be better suited for mobile measurements as needed in campaigns. The current enclosure was designed for stationary use and gives proof of the concept. Nevertheless, there is a high demand to use the enclosure for campaigns. This raises a whole new set of requirements such as reduced weight, size and power consumption.

6   Conclusion

We designed, engineered, assembled, and successfully tested an automated enclosure for atmospheric solar-tracking instruments, in our case *EM27/SUNs*, under extreme weather conditions. The automated solar-tracking system is located in central Munich (48.15N, 11.57E).

The enclosure is suited for fully autonomous operation and enables easy handling of the measurement system. When potentially poor weather conditions arise, the system can be shut down and protected within seconds. In case of sudden rain, the

enclosure reliably protects the measurement system by closing its cover. In this manner, the measurement system is sheltered from heavy storms, rainfalls, and snowfalls without need of any physical human interaction.

Remote access can be obtained by any smartphone or computer. Thus, the system can be observed and controlled from anywhere in the world. This considerably lowers the inhibition level to start measurements, resulting in a significant increase in the amount of data collected. Furthermore, the automated enclosure reduces the need for costly human effort and optimizes the chance to sample good data, even during periods of instable weather conditions. Accordingly, the measurement system has a much higher efficiency, which should increase the significance of any scientific outcome derived from these data.

In sum, the enclosure provides the main functionality for a complete automation of the measurement system, guarantees maximization of the amount of data collected while minimizing the operational risks and costs, thus providing a foundation for long-term GHG monitoring sensor network.

Acknowledgments. We gratefully thank Gerold Wunsch for helping with the cover concept development. We also acknowledge our Bruker colleagues Peter Maas, Gregor Surawicz for technical support. Further, we thank Florian Dietrich, Frank Hase, Bruce Daube, Steven C. Wofsy, Andreas Meichelböck, Johannes C. Paetzold, Duc Hai Nguyen, and Patrick Aigner for fruitful discussions and Stephen Starck from the TUM language center for the helpful English editing.

Jia Chen is supported by Technische Universität München - Institute for Advanced Study, funded by the German Excellence Initiative and the European Union Seventh Framework Programme under grant agreement n° 291763.

References

Bruker Optic GmbH: IFS 125 User Manual, http://spec.jpl.nasa.gov/ftp/pub/outgoing/IFS125HR_manual.pdf, 2006.

Butz, A., Dinger, A. S., Bobrowski, N., Kostinek, J., Fieber, L., Fischerkeller, C., Giuffrida, G. B., Hase, F., Klappenbach, F., Kuhn, J., Lübcke, P., Tirpitz, L., and Tu, Q.: Remote sensing of volcanic CO_2, HF, HCl, SO_2, and BrO in the downwind plume of Mt. Etna, Atmospheric Measurement Techniques, 10, 1–14, doi:10.5194/amt-10-1-2017, https://www.atmos-meas-tech.net/10/1/2017/, 2017.

Chen, J., Viatte, C., Hedelius, J. K., Jones, T., Franklin, J. E., Parker, H., Gottlieb, E. W., Wennberg, P. O., Dubey, M. K., and Wofsy, S. C.: Differential Column Measurements Using Compact Solar-Tracking Spectrometers, Atmospheric Chemistry and Physics, doi:10.5194/acp-2015-1058, 2016.

Chen, J., Nguyen, H., Toja-Silva, F., Heinle, L., Hase, F., and Butz, A.: Power Plant Emission Monitoring in Munich Using Differential Column Measurements, in: EGU General Assembly Conference Abstracts, vol. 19 of *EGU General Assembly Conference Abstracts*, p. 16423, 2017.

Franklin, J. E., Jones, T., Floerchinger, C. R., Hajny, K. D., Parker, H. A., Heinle, L., Paetzold, J., Lavoie, T. N., Wofsy, S. C., Chen, J., Shepson, P. B., Mielke, L. H., Richardson, S., Davis, K. J., Gottlieb, E., Budney, J., Dubey, M. K., and Hase, F.: Multi-scale Top-down Closure of CH_4 & CO_2 Sources in Indianapolis using Distributed Column and in situ Airborne and Tower Measurements, AGU Fall Meeting Abstracts, 2016.

Frey, M., Hase, F., Blumenstock, T., Groß, J., Kiel, M., Mengistu Tsidu, G., Schäfer, K., Sha, M., and Orphal, J.: Calibration and instrumental line shape characterization of a set of portable FTIR spectrometers for detecting greenhouse gas emissions, Atmospheric Measurement Techniques, 8, 3047–3057, 2015.

Geibel, M. C., Gerbig, C., and Feist, D. G.: A new fully automated FTIR system for total column measurements of greenhouse gases, Atmospheric Measurement Techniques, 3, 1363–1375, doi:10.5194/amt-3-1363-2010, https://www.atmos-meas-tech.net/3/1363/2010/, 2010.

Gisi, M., Hase, F., Dohe, S., and Blumenstock, T.: Camtracker: a new camera controlled high precision solar tracker system for FTIR-spectrometers, Atmospheric Measurement Techniques, 4, 47–54, doi:10.5194/amt-4-47-2011, 2011.

Gisi, M., Hase, F., Dohe, S., Blumenstock, T., Simon, A., and Keens, A.: XCO_2-measurements with a tabletop FTS using solar absorption spectroscopy, Atmospheric Measurement Techniques, 5, 2969–2980, 2012.

Hase, F.: Improved instrumental line shape monitoring for the ground-based, high-resolution FTIR spectrometers of the Network for the Detection of Atmospheric Composition Change, Atmospheric Measurement Techniques, 5, 603–610, doi:10.5194/amt-5-603-2012, https://www.atmos-meas-tech.net/5/603/2012/, 2012.

Hase, F., Frey, M., Blumenstock, T., Groß, J., Kiel, M., Kohlhepp, R., Mengistu Tsidu, G., Schäfer, K., Sha, M., and Orphal, J.: Application of portable FTIR spectrometers for detecting greenhouse gas emissions of the major city Berlin, Atmospheric Measurement Techniques, 8, 3059–3068, 2015.

Hase, F., Frey, M., Kiel, M., Blumenstock, T., Harig, R., Keens, A., and Orphal, J.: Addition of a channel for XCO observations to a portable FTIR spectrometer for greenhouse gas measurements, Atmospheric Measurement Techniques, 9, 2303–2313, doi:10.5194/amt-9-2303-2016, https://www.atmos-meas-tech.net/9/2303/2016/, 2016.

Hedelius, J. K., Viatte, C., Wunch, D., C., R., Toon, G. C., Chen, J., Jones, T., Wofsy, S. C., Franklin, J. E., Parker, H., Dubey, M., and Wennberg, P. O.: Assessment of errors and biases in Xgas retrieved from a low resolution spectrometer (EM27/SUN), submitted to Atmospheric Measurement Techniques, amt-2016-39, initial submission, 2016.

K.K., H. P.: InGaAs Photodiodes, https://www.hamamatsu.com/resources/pdf/ssd/ingaas_kird0005e.pdf, 2015.

Klappenbach, F., Bertleff, M., Kostinek, J., Hase, F., Blumenstock, T., Agusti-Panareda, A., Razinger, M., and Butz, A.: Accurate mobile remote sensing of XCO_2 and XCH_4 latitudinal transects from aboard a research vessel, Atmospheric Measurement Techniques, 8, 5023–5038, 2015.

5 LLC, T. J. T.: Indium Gallium Arsenide Detectors, http://www.judsontechnologies.com/files/pdf/InGaAs_shortform_DEC2004_rev2.pdf, 2004.

Neefs, E., De Mazière, M., Scolas, F., Hermans, C., and Hawat, T.: BARCOS, an automation and remote control system for atmospheric observations with a Bruker interferometer, Review of Scientific Instruments, 78, 035109, doi:http://dx.doi.org/10.1063/1.2437144, http://scitation.aip.org/content/aip/journal/rsi/78/3/10.1063/1.2437144, 2007.

10 Sha, Dr. M. K.: Glass dome selection as a cover for protecting remote sensing instruments performing atmospheric measurements of trace gases, Technical notes, Karlsruhe, Karlsruher Institut für Technologie (KIT), 2015.

Toja-Silva, F., Chen, J., Hachinger, S., and Hase, F.: {CFD} simulation of {CO2} dispersion from urban thermal power plant: Analysis of turbulent Schmidt number and comparison with Gaussian plume model and measurements, Journal of Wind Engineering and Industrial Aerodynamics, 169, 177 – 193, doi:https://doi.org/10.1016/j.jweia.2017.07.015, http://www.sciencedirect.com/science/article/pii/S0167610517302258, 2017.

Toon, G., Blavier, J.-F., Washenfelder, R., Wunch, D., Keppel-Aleks, G., Wennberg, P., Connor, B., Sherlock, V., Griffith, D., Deutscher, N., et al.: Total column carbon observing network (TCCON), in: Fourier Transform Spectroscopy, p. JMA3, Optical Society of America, 2009.

Viatte, C., Lauvaux, T., Hedelius, J. K., Parker, H., Chen, J., Jones, T., Franklin, J. E., Deng, A. J., Gaudet, B., Verhulst, K., Duren, R., Wunch,
20 D., Roehl, C., Dubey, M. K., Wofsy, S., and Wennberg, P. O.: Methane emissions from dairies in the Los Angeles Basin, Atmospheric Chemistry and Physics, 17, 7509–7528, doi:10.5194/acp-17-7509-2017, https://www.atmos-chem-phys.net/17/7509/2017/, 2017.

Wunch, D., Toon, G. C., Blavier, J. F., Washenfelder, R. A., Notholt, J., Connor, B. J., Griffith, D. W., Sherlock, V., and Wennberg, P. O.: The total carbon column observing network, Philos Trans A Math Phys Eng Sci, 369, 2087–112, 2011.